Temporal variability of P-wave attenuation due to gas bubbles in a marine sediment

M. D. J. Tuffin[1], A. I. Best[2], J. K. Dix[1], J. M. Bull[1]

[1] School of Ocean and Earth Sciences, University of Southampton, Southampton Oceanography Centre, Southampton, SO14 3ZH, UK. mdjt@soc.soton.ac.uk

[2] Challenger Division for Seafloor Processes, Southampton Oceanography Centre, Southampton, SO14 3ZH, UK. aib@soc.soton.ac.uk

Abstract

Acoustic attenuation measurements in gassy intertidal sediments in Dibden Bay, Southampton Water (UK) show significant and systematic changes over a tidal cycle. Modelling of the attenuation-frequency response curves, based on extant theory with modifications for hydrostatic pressure/gas bubble size relations and bubble size distributions, reproduces the observations over the tidal cycle. However, more work is needed to constrain the model input parameters to verify the theory more completely, particularly bubble size distribution and morphology.

1. Introduction

Zones of poor acoustic penetration and high reflection/backscatter amplitudes are observed in many shallow marine sediments, that is those less than 20 m sub-seafloor depth. This "acoustic turbidity" is caused by the presence of free gas bubbles, principally methane, that result in high attenuation and low velocity of transmitted signals relative to those transmitted through fully water saturated sediments [1].

The presence of methane, and smaller amounts of other gases, in shallow sediments is thought to be the result of anaerobic bacterial decomposition of organic matter [2]. In the marine environment, sediment pore water is rich in sulphates, allowing sulphate-reducing bacteria to dominate and produce hydrogen sulphide. Once the sulphates have been depleted, carbonate-reducing bacteria can compete more efficiently, and begin methane production [3].

Knowledge of gassy sediment properties is of interest to a number of offshore activities, including drilling operations and the siting of seafloor structures [4]. Slope stability is an area of concern to offshore operators who are working increasingly in the deep waters of the continental slope (water depths 200 – 2000 m). Evidence for gassy sediments (e.g. pockmarks [5]) and gas hydrates are commonly found adjacent to large, historical, submarine landslides [6], and, although the causes of submarine landslides are poorly understood at present, it is known that the presence of gas bubbles lowers the shear strength of a marine sediment [7]. Remote sensing of the seabed and sub-seabed using high-resolution acoustic methods promotes the possibility of inverting acoustic data for the geotechnical parameters needed in the above applications. However, a better understanding of acoustic propagation mechanisms in both fully saturated and gassy marine sediments is required to achieve this goal.

Acoustic turbidity was observed on chirp (2 – 8 kHz) sub-bottom profiles of the intertidal zone at Dibden Bay, Southampton Water (UK), and this site was subsequently chosen for a series of more detailed experiments [8]. This paper presents the preliminary results of an *in situ* acoustic transmission experiment conducted on the gassy sediments found at this site and provides a basis for validating existing models. The experiment used a vertical hydrophone array and a mini-boomer sound source to monitor acoustic attenuation over one complete tidal cycle. The effect of hydrostatic pressure on bubble size and the associated acoustic response was modelled using the theory of Anderson and Hampton [9, 10] with some enhancements. These were introduced to account for both the effects of variable bubble size and bubble size distribution. The outputs from the model were compared to the *in situ* P-wave transmission data.

The results show that *in situ* acoustic attenuation is sensitive to hydrostatic pressure and is broadly well described by the model. However, further work is needed to constrain the model input parameters, especially bubble size distribution, total gas volume and sediment shear strength. This will be achieved by collecting pressurised sediment cores at the site in the near future and by subsequent laboratory analyses.

2. The Anderson and Hampton model

Anderson and Hampton [9, 10] developed a model to predict the effects of shallow gas on the attenuation and velocity characteristics of gassy sediments, based on the theory of gas bubble resonance in water. They concluded

TG Leighton, GJ Heald, HD Griffiths, G Griffiths, (eds.), 'Acoustical Oceanography', Proc. Institute of Acoustics Vol. 23 Part 2, 2001.

that bubble resonance frequency depends upon the bubble radius, the thermal properties of the gas, the dynamic shear modulus and bulk density of the sediment, and the ambient hydrostatic pressure. Therefore, knowledge of a bubble resonance frequency, for example, could be used to derive information on the radius of the bubble or the dynamic shear modulus of the saturated sediment. Bubble resonance has a significant effect on acoustic propagation and three distinct states may be identified: the insonifying frequency may be below, at/near or above the resonance frequency. Each state has its own characteristic sound speed, c, and attenuation, a, predicted by the model. A typical set of input parameters and their values, either measured from samples recovered from the Dibden Bay site or taken from the literature, are given in Table 1. Values of the remaining parameters required by the model not mentioned in the table (A, the gas polytropic coefficient; P_0, the ambient hydrostatic pressure; K, the bulk modulus of the saturated sediment; c_0, the P-wave velocity in the gas free sediment; ρ_w, water density; damping coefficients δ_r, δ_t, δ_f) may be measured, calculated or estimated from the literature [9-12].

Sediment porosity, n	0.61
Saturated sediment density, ρ_{sat}	1475 kg / m^3
Mineral bulk modulus, K_m	3.6×10^{10} N / m^2 †
Frame bulk modulus, K_f	1.389×10^9 N / m^2 ‡
Interstitial water bulk modulus, K_w	2.24×10^9 N / m^2
Dynamic shear modulus, G	2.813×10^5 N / m^2 †
Imaginary part of dynamic shear modulus, G'	1×10^4 N / m^2
Bubble radius, r	$0.01 - 10 \times 10^{-3}$ m
Gas porosity, n_g	0.0001, 0.001, 0.01
Gas density, ρ_g	0.717 kg / m^3 at STP
Specific heat at constant pressure of gas, S_p	2.19 J / kg.°C
Thermal conductivity of gas, C_g	3.11×10^{-2} J / s.m.°C
Ratio of the specific heats of the gas, γ	1.31

† from [11]

‡ from [13]

Table 1. Values of parameters used in the model

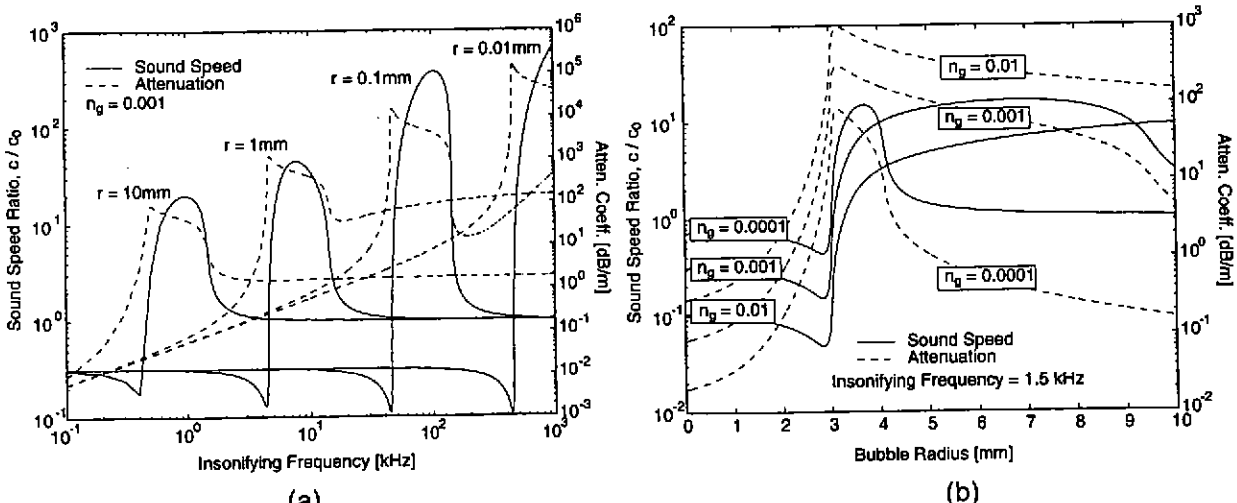

Figure 1. Model results of sound speed ratio, c/c_0, and attenuation, a, for (a) constant bubble radius, r, and gas porosity, n_g, versus insonifying frequency, f, and (b) constant insonifying frequency, f, and gas porosity, n_g, versus bubble radius, r.

The model results in Figure 1 show that if the insonifying frequency is lower than the resonance frequency then the sound speed ratio, c/c_0, is less than unity. This would indicate a gassy sediment sound speed less than its gas free equivalent. A transition zone is seen at frequencies near resonance: the sound speed ratio dramatically increases before gradually approaching a value of 1.0 when the resonance zone is exceeded. The bubbles also cause a dramatic increase in attenuation at frequencies near resonance. This is thought to be a result of the large increase in scattering cross section of the bubble at resonance [9]. Note that the attenuation calculated here does

not include contributions from the intrinsic attenuation (absorption) of the sediment. Smaller bubbles require a higher insonifying frequency to make them resonate (Figure 1a) and a single insonifying frequency will cause resonance only in a narrow range of bubble radii (Figure 1b). In a real sediment there will be a variety of bubble sizes present. Hence, bubble resonances might be detected across a broad frequency range.

3. *In situ* measurements

3.1 Experimental set-up

In situ transmission measurements were obtained during March 2000 at Dibden Bay, an intertidal mudflat situated on the eastern shore of the upper reaches of Southampton Water (UK). The site is composed of very soft mud with a surficial shell layer in some areas. Evidence of free gas may be inferred from acoustic turbidity on chirp reflection profiles (Figure 2a) and the odour of hydrogen sulphide in the mud – an indicator of the anoxic conditions required by methanogenic bacteria. The site chosen for the experiment, an area with a surficial shell layer, may be seen in the chirp reflection profile (Figure 2a) as the domed area of high amplitude reflections. It is assumed that the gas layer, seen as the reflector about 1 ms below the seabed, extends under this shelly zone. The experiment used a mini-boomer acoustic source and a vertical array of four hydrophones placed at strategic depths within the sediment 1m from the source (Figure 2b). The mini-boomer uses a high-voltage inverter to drive a magneto-propulsive plate 20 cm in diameter and tests have shown that it produces a repeatable signal, a spherical radiation pattern and a spectral content between 0-11 kHz notched at about 2.5 kHz; the hydrophones show a flat frequency response up to 10 kHz [14]. The depths were chosen to ensure that there was at least one hydrophone above the gas horizon and at least one below, as inferred from chirp reflection profile data (Figure 2b). The mini-boomer was fired at ten-minute intervals over the period of a tidal cycle. The data were recorded using a digital storage oscilloscope and tidal height was calculated from tide gauge data collected routinely around the port of Southampton.

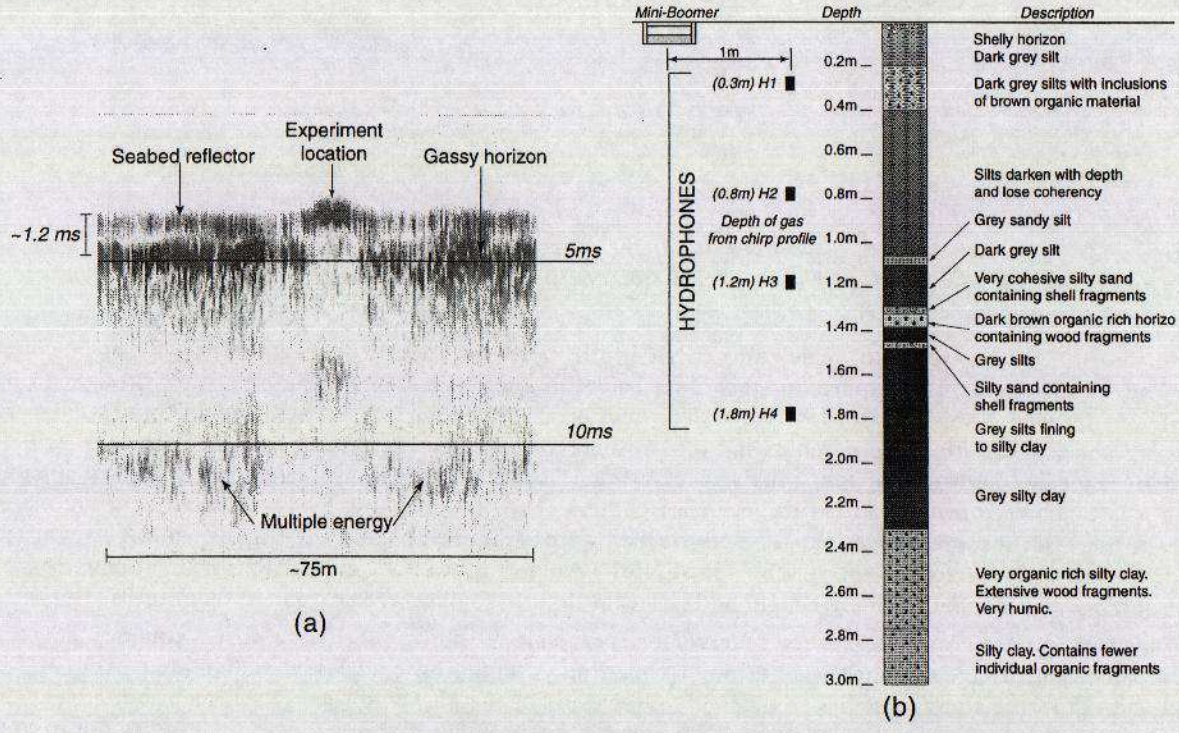

Figure 2. (a) Chirp reflection profile showing experiment location, seabed reflector and gassy horizon, and (b) positions of hydrophones within the sediment column.

3.2 Data processing

The data were processed using a filter correlation technique [15], which involves filtering the signal and a reference with a series of band pass filters, each with a width of 100 Hz, from a minimum central frequency of 100 Hz to an arbitrarily determined maximum central frequency of 2 kHz. Attenuation coefficients for each frequency band were calculated using the log spectral ratio method (Equation 1) with a spherical spreading law. Two reference signals were used, those signals received at hydrophones H1 and H2. Each shot was processed in the same manner.

$$a(f)=\frac{8.686}{\delta x}\ln\left|\frac{A_{ref}}{A_{sig}}.\frac{x_{ref}}{x_{sig}}\right| \quad (1)$$

where $a(f)$ is the attenuation coefficient [dB/m]; $A_{ref,sig}$ are the root mean square energies of the filtered reference and signal time series, respectively; $x_{ref,sig}$ are the source receiver separations in metres for the reference and signal time series, respectively; and δx is the $x_{sig} - x_{ref}$.

3.3 Results

Shot gathers for low and high water (Figure 3a,b) indicate a change in the character of the received signal both with tidal height and hydrophone depth.

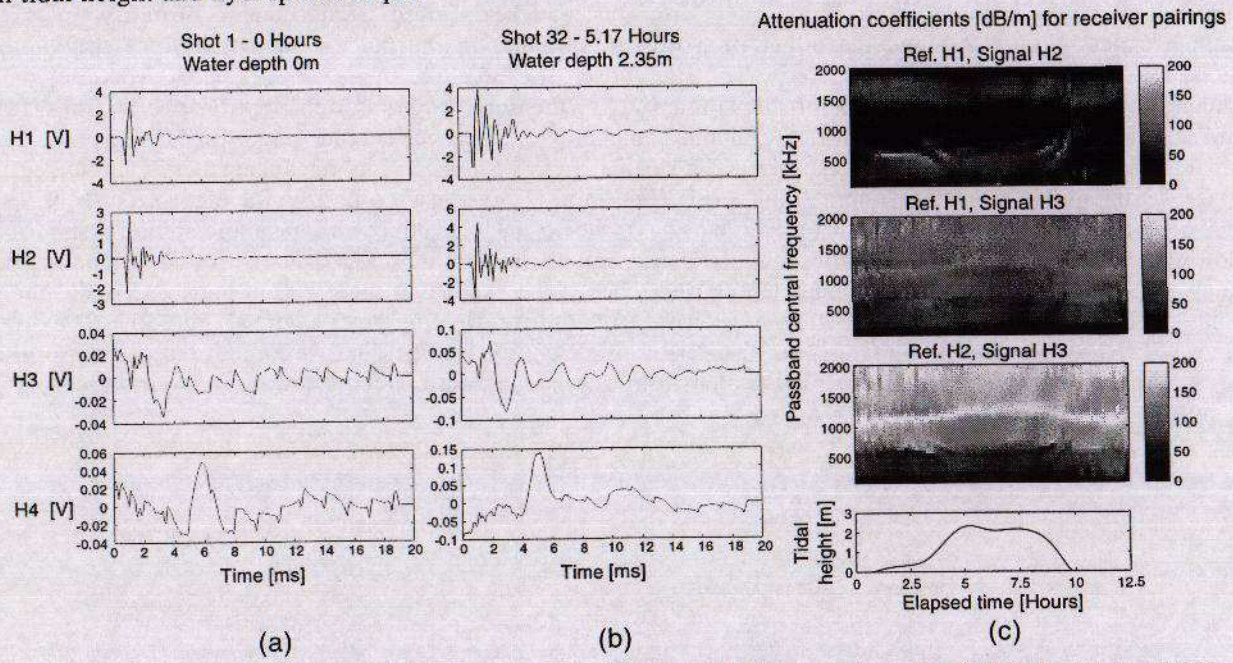

Figure 3. Self normalised shot gathers at (a) the start of the experiment and (b) the highest tide during the experiment. (c) Calculated attenuation coefficients for various reference/signal pairings.

A deterioration in the signal to noise ratio (SNR) with increasing depth of receiver is evident in both shot gathers. The spikes occurring at approximately 2 ms intervals on H3 and H4 in Figure 3a are thought to be the results of interference from the oscilloscope power supply. There is a clear drop in signal amplitude between receivers H2 and H3 in both gathers, indicating the presence of a highly attenuating zone between the two. There is little difference in amplitude of the signals received at H1 and H2. An improvement in SNR with increasing tidal height is evident from H3 and H4 in both shot gathers. The signals show less influence from the electrical noise due to the oscilloscope power supply with deeper water (Figure 3b) and the highest voltage recorded for each hydrophone is in excess of those seen for shallow water (Figure 3a), indicating lower attenuation of the signal. Problems with the data from hydrophone H4 meant that these data were excluded from the analysis.

Calculated attenuation coefficients for receiver reference/signal pairs, plotted against frequency and time in Figure 3c, show an influence of tidal height on attenuation. Attenuation coefficients calculated using H2 as the reference and H3 as the source (i.e. those receivers either side of the gassy/non-gassy sediment boundary) show a comparatively low attenuation zone below 600 Hz and a high attenuation zone above, peaking at approximately 1.1 – 1.4 kHz. The values of attenuation are very high (greater than 200 dB/m at 1 kHz) suggesting that attenuation caused by bubble resonance and scattering is occurring at these frequencies. This attenuation peak increases in frequency in response to an increase in tidal height.

4. The effects of hydrostatic pressure on a gassy sediment

A comparison of the experimental and model results in Sections 2 and 3 suggest the increase in resonance frequency with tidal height is due to a decrease in bubble radius. The driving mechanism for this bubble radius decrease is a change in hydrostatic pressure, which will affect the internal bubble pressure as the system equilibrates, and hence, bubble radius.

4.1 Pressure equilibrium

Direct measurement of the pressure inside each individual bubble is not practical so an estimate must be made by considering the conditions in the surrounding saturated sediment matrix. The following limits on the internal pressure, u_g, were proposed by Wheeler *et al.* [16].

$$u_w + \frac{2T}{R_{\max}} \leq u_g \leq u_w + \frac{2T}{R_{\min}}, \tag{2}$$

where u_w is the pore water pressure; T is the surface tension; R_{max}, R_{min} are the limiting values of radius of curvature of meniscus (see [16] for details). The pore pressure at the depth of interest (approximately 1m) is taken as hydrostatic for simplicity [17], although it is important to note that a more accurate model of tidally induced pore pressure is available [18]. Surface tension effects are small compared to the pore pressure depending on the bubble radius: for a bubble radius of 0.1 mm and a surface tension coefficient of 0.073 N/m (the value for an air/water mixture), surface tension amounts to 1.46 kN/m^2; for a bubble radius of 1 mm the surface tension amounts to 146 N/m^2. The available evidence suggests that bubble radii are generally in excess of 0.1 mm [19], [20] and the frequency range of the processed data will be restricted to below 2 kHz, well below the resonance frequency of a 0.1mm bubble, so surface tension effects will be ignored here.

It is also assumed that the increase in pore pressure at the depth of the gas is instantaneous with the increase in hydrostatic pressure. Since the pressure inside the bubble equilibrates with the surrounding conditions there must be a similar increase in the internal pressure of the bubble. In the absence of any mass transfer into the bubble there is a decrease in bubble volume, and hence bubble radius. This change in bubble radius will result in a change in resonance frequency of the system. Assuming the gas conforms to the Ideal Gas Law and there is no temperature within the sediment change during the adjustment, the final bubble radius, r_1, may be calculated from:

$$r_1^3 = \frac{P_0}{P_1} . r_0^3, \tag{3}$$

where r_0 is the initial bubble radius; and P_0, P_1 are the initial and final pressures respectively. A decrease in hydrostatic pressure will result in an increase in bubble radius using the same argument.

4.2 Gas diffusion

The following model for predicting the radius $R(t)$ of a growing bubble was proposed by Boudreau *et al.* [21]:

$$R(t) = \left[\frac{nD}{2c_g} \left\{ \frac{SR_1^2}{3D} + (c_1 - c_0) \right\} t + R_0^2 \right]^{1/2}, \tag{4}$$

Where n is the porosity; D is the tortuosity-corrected diffusivity; c_g is the concentration of gas in the bubble; S is the local rate of methanogenesis; R_1 is the separation distance between bubbles ($R_1 \gg R$); c_1 is the ambient concentration of the gas; c_0 is the pore water concentration of the gas at R and is a function of c_g; t is the time; R_0 is the initial radius of the bubble. Consider a gas bubble at equilibrium with the surrounding water saturated sediment. A small reduction in bubble volume, such as that caused by an increase in hydrostatic pressure, will lead to a small increase in c_g (small enough that $c_0 \leq c_1$); diffusion will act to slow down the rate of bubble growth. However, a large reduction in bubble volume (and associated increase in c_g) will lead to sediment undersaturation ($c_0 > c_1$) that may outweigh the local rate of gas production (methanogenesis); this will result in a net reduction in bubble volume and radius. If there in insufficient undersaturation the bubble will continue to grow, albeit at a slower rate.

With sufficient chemical data it should be possible, using this model, to calculate the effect of increasing c_g on the radius of the bubble, but in the absence of this data in this study it has been decided to assume that there is no net change of the bubble radius due to diffusion.

4.3 Bubble size distribution

X-ray computed tomography (CT) scans of gassy sediment cores [20] show that a range of bubble sizes is the norm, with each bubble size population having its own associated gas porosity. Sediment coring at Dibden Bay and X-ray CT scans are planned for the near future, but for the purposes of this work a series of gas porosities were assigned to a set of arbitrarily determined bubble radii. Attenuation coefficients were calculated for each bubble radius using (1) to (9) and the input parameters in Table 1. The total attenuation due to the bubble size distribution is found by summing the individual bubble size attenuation coefficients at each insonifying frequency.

4.4 Model implementation

The model was implemented as a function of hydrostatic pressure using the tidal height curve obtained during the acoustic transmission experiment at Dibden Bay. The increment in hydrostatic pressure caused by the tide was used to calculate the bubble shrinkage/expansion due to pressure equilibrium and this new radius was used to calculate the attenuation coefficients over an arbitrarily defined frequency range (100 – 2000 Hz). The sequence was repeated for each subsequent tidal increment, equivalent to one sample interval of 10 minutes. The attenuation contribution from each bubble size was calculated in this manner for the whole tidal cycle, and then these single bubble size components were summed to give the total attenuation of the arbitrary bubble size distribution, according to Section 4.3. The arbitrary bubble size distribution was adjusted to obtain the best fit to the *in situ* data, the final distribution shown in Figure 4.

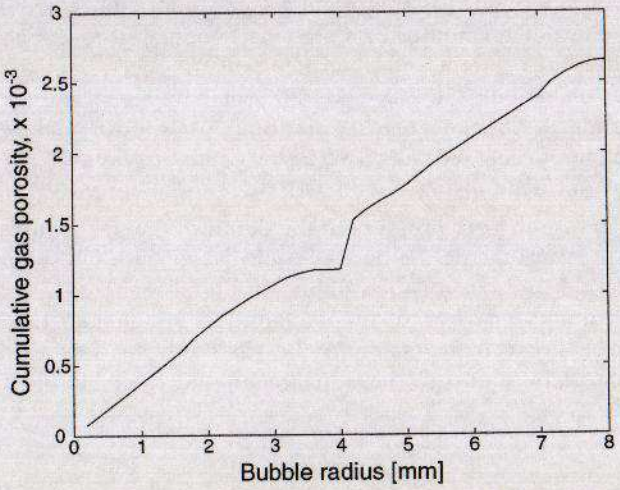

Figure 4. Cumulative gas porosity versus bubble radius

5. Results and Discussion

It can be seen from the *in situ* results and the model results shown in Figure 5a that hydrostatic pressure (expressed here as tidal height) has a marked effect on dominant resonance frequency, because the only compressible components of the sediment at these pressures are the gas bubbles. The *in situ* data show an increase in resonance frequency from approximately 1150 Hz to approximately 1250 Hz as the tidal height over the site increases. Our model reproduces this observation, and although the dominant resonance frequencies predicted are slightly lower than those seen in the *in situ* data, the increase seen is of a similar size (Figure 5b). The model results match the magnitude and shape of the attenuation profiles adequately in the 600 – 1400 Hz range, especially for the 0.38 m tidal height. The model varies from the *in situ* data by less than 10% in this region with the exception of the points at 700 Hz and 1150 Hz, the attenuation peaks in the *in situ* data.

Differences between the model results and the *in situ* data can be explained by a number of factors. A lack of quantitative geotechnical measurements, except for some basic porosity and density measurements, means that several of the input values had to be estimated or calculated from other sources. Most importantly, there was no data available for the bubble size distribution within the sediment, so a series of values, as shown in Figure 4, were hypothesised and adjusted to best approximate the *in situ* data.

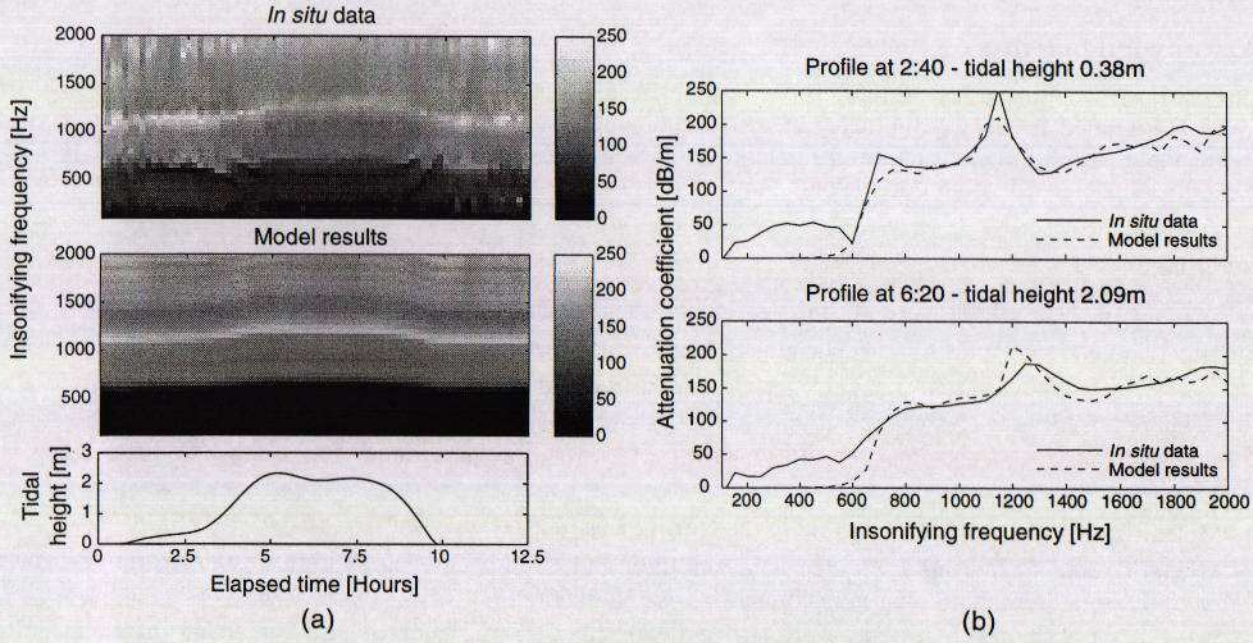

Figure 5. Attenuation coefficients (a) over a whole tidal cycle for the in situ data and the model, and (b) for tidal heights of 0.38 m and 2.09 m.

The various assumptions made will have an effect on the final model result with the most important being the internal bubble pressure. The lack of any information concerning the local rate of methanogenesis and concentrations of methane in the pore water and bubbles means that any diffusive component is impossible to estimate. The impracticality of measuring the pressure inside an individual gas bubble buried in sediment without disturbing the bubble means that other methods to establish an internal pressure must be made. Calculations based on indirect measurements have been undertaken [22], but the problem of sediment disturbance remain and relating gas pressure to pore pressure, as presented here, also introduces problems. Pore pressure has been assumed to be the hydrostatic pressure at the gas horizon. This is clearly a simplification of the problem, and further improvements could be made to the model by calculating the tidally induced pore pressure more accurately and accounting for the effect of the presence of gas, as has been described in [18]. Despite these assumptions, the model shows good correlation with the *in situ* data in terms of the time at which the dominant resonance frequency changes and the shape of the curve. It should be noted, however, that the attenuation coefficients calculated in the model do not include the intrinsic attenuation due to the fully saturated sediment.

The model results indicate that, by matching model output to *in situ* acoustic data and using accurate geotechnical data, an estimation of the bubble size distribution within the sediment may be made. Further constraining the gas pressure could make improvements, although results here show a reasonable estimate. This bubble size distribution may be used to calculate the bulk gassy sediment geotechnical properties using relationships such as those presented in [23].

6. Conclusions

The Anderson and Hampton model [9, 10] was used to predict the change in the attenuation-frequency response of the gassy marine sediments in Dibden Bay due to changes in tidal height. The effect of changing hydrostatic pressure on gas bubbles contained within the sediment was modelled by considering pressure equilibrium between the bubble and the surrounding pore water. A bubble size distribution was estimated, the attenuation due to each bubble size/gas porosity pair was calculated and the total attenuation was obtained from the sum of the individual components. The model output shows good correlation with the *in situ* data, although improvements could be made by further constraining methods for assessing the internal bubble pressure. The agreement seen suggests that bubble size distributions may be estimated with knowledge of water saturated sediment geotechnical properties and *in situ* acoustic measurements. Further work is planned to constrain these parameters.

7. Acknowledgements

This work is supported by Natural Environment Research Council studentship number GT04/98/272/ES. Thanks are extended to Gary Robb and Simon Dean for their assistance in collecting the *in situ* data, to Andy Harris for the design and construction of the mini-boomer system and to Bernie Boudreau for his advice. Finally, thanks go to Associated British Ports (Southampton) for granting access to the field site and for the tide data.

References

[1] Schubel JR. Natural Gases in Marine Sediments. Plenum, New York, 1974, pp. 275-298

[2] Floodgate GD and Judd AG. The origins of shallow gas. *Cont. Shelf Res.* 1992; **12**: 1145-1156

[3] Rice DD and Claypool GE. Generation, accumulation, and resource potential of biogenic gas. *AAPG Bull.* 1981; **65**: 5-25

[4] Sills GC and Wheeler SJ. The significance of gas for offshore operations. *Cont. Shelf Res.* 1992; **12**: 1239-1250

[5] McQuillin R and Fannin N. Explaining the North Sea's lunar floor. *New Scientist* 1979; **83**: 90-92

[6] Mienert J and Posewang J. Evidence of shallow- and deep-water gas hydrate destabilizations in North Atlantic polar continental margin sediments. *Geo-Marine Letters* 1999; **19**: 143-149

[7] Whelan III T, Coleman JM, Roberts HH and Suhayda JN. The occurrence of methane in recent deltaic sediments and its effect on soil stability. *Bull. Int. Assoc. Eng. Geol.* 1976; **14**: 55-64

[8] Tuffin MDJ, Best AI, Dix JK and Bull JM. Acoustic characterisation of gassy marine sediments in Dibden Bay, Southampton Water (UK), in *Proc. 5th European Conference on Underwater Acoustics,* 2000, pp. 825-830

[9] Anderson AL and Hampton LD. Acoustics of gas bearing sediments I. Background. *J. Acoust. Soc. Am.* 1980; **67**: 1865-1889

[10] Anderson AL and Hampton LD. Acoustics of gas bearing sediments II. Measurements and models. *J. Acoust. Soc. Am.* 1980; **67**: 1890-1903

[11] Wilkens RH and Richardson MD. The influence of gas bubbles on sediment acoustic properties: *in situ*, laboratory and theoretical results from Eckernförde Bay, Baltic Sea. *Cont. Shelf Res.* 1998; **18**: 1859-1892

[12] Gassmann F. Elastic waves through a packing of spheres. *Geophys.* 1951; **16**: 673-685

[13] Hamilton EL. Elastic properties of marine sediments. *J. Geophys. Res.* 1971; **76**: 579-604

[14] Best AI, Huggett QJ and Harris AJK. Comparison of *in situ* and laboratory acoustic measurements on Lough Hyne marine sediments. Submitted to *J. Acoust. Soc. Am.*.

[15] Courtney RC and Mayer LA. Calculation of acoustic parameters by a filter-correlation method. *J. Acoust. Soc. Am.* 1993; **93**: 1145-1154

[16] Wheeler SJ, Sham WK and Thomas SD. Gas pressure in unsaturated offshore soils. *Can. Geotech. J.* 1990; **27**: 79-89

[17] Craig RF. Soil Mechanics. Chapman and Hall, London, 1992, pp 80-85.

[18] Wang K, Davis EE and van der Kamp G. Theory for the effects of free gas in subsea formations on tidal pore pressure variations and seafloor displacements. *J. Geophys. Res.* 1998; **103**: 12339-12353

[19] Gardner TN and Goringe MJ. The measurement of gas bubble size distributions in a three phase laboratory gassy soil. *Geotech. Test. J.* 1988; **11**: 49-55

[20] Anderson AL, Abegg F, Hawkins JA, Duncan ME and Lyons AP. Bubble populations and acoustic interaction with the gassy floor of Eckernförde Bay. *Cont. Shelf Res.* 1998; **18**: 1807-1838

[21] Boudreau BP, Gardiner B, Johnson, B. Rate of growth of isolated bubbles in sediments with a distributed diagenetic source of methane. Submitted to *Limnol. Oceanogr.*.

[22] Whelan III T, Ishmael JT and Rainey GB. Gas-sediment interactions in Mississippi Delta sediments, in *Proc. 10th Annual Offshore Technology Conference* 1978, pp. 1029-1036.

[23] Wheeler SJ and Gardner TN. Elastic moduli of soils containing large gas bubbles. *Géotech.* 1989; **39**: 333-342